Photogrammetrie • Fernerkundung • Geoinformation 4/2003, S. 317–326, 6 Fig., 3 Tab.

From Airborne Digital Raw Data to Image Maps

Rupert Müller, Gintautas Palubinskas, Peter Reinartz, Manfred Schroeder, Volker Amann & Rolf Stätter, Oberpfaffenhofen

Keywords: aerial photogrammetry, airborne scanner data, direct georeferencing, radiometric correction, mosaicking, image maps

Zusammenfassung: *Flugzeug-Scannerdaten: Von digitalen Rohdaten zu Orthobildern*. In den letzten Jahren werden bei Anwendungen der Flugzeugfernerkundung, unter anderem für die Nutzung in Geographischen Informationssystemen, immer häufiger zusammenhängende Bildkarten als einzelne Bildstreifen verwendet. Die häufigsten Probleme während des Mosaiking Prozesses sind bedingt durch Fehler bei der Ortho-Rektifizierung, durch radiometrische Unterschiede in den einzelnen Bildstreifen quer zur Flugrichtung sowie zwischen den einzelnen Streifen. Die vorgeschlagene Prozedur für die Erstellung von ortho-rektifizierten Bildkarten besteht daher aus drei Schritten. Für die einzelnen Bildstreifen wird zunächst eine Normalisierung mit Hilfe einer bildbasierten empirischen Korrekturmethode, welche sämtliche blickwinkelabhängigen Effekte berücksichtigt, durchgeführt. Die einzelnen Bildstreifen werden anschließend mit Hilfe der aufgezeichneten Lage- und Positionsdaten des IGI *CCNS*/*AEROcontrol-IIb* Systems, einem digitalen Höhenmodel und der Methode der direkten Georeferenzierung ortho-rektifiziert. Um die Unterschiede zwischen den einzelnen Bildstreifen zu korrigieren, wird eine radiometrische Korrekturmethode verwendet, die die Bildinformation in den Überlappungsbereichen der Streifen benutzt. Die Anwendungen auf Daten des multispektralen Flugzeugscanners DAEDALUS *AADS 1286 ATM* zeigen die Effektivität und die Nutzungsmöglichkeiten der vorgeschlagenen Methodik besonders für die thematische Analyse und die Integration der Daten in ein GIS.

Summary: Recent airborne remote sensing applications show a tendency from an interpretation of single image strips to an evaluation of extended image maps for further usage in data fusion and GIS applications. Most of the problems during the mosaicking process are caused by geometric ortho-rectification errors, radiation variations across the single image strips and between adjacent image strips. The proposed procedure for generating ortho-rectified image maps consists of the following three steps. Within an image strip radiometric normalization is performed using an image-based empirical radiometric correction method, which accounts for sensor viewing angle effects. Individual strips are then ortho-rectified applying the direct georeferencing approach by using the onboard IGI *CCNS*/*AEROcontrol-IIb* system for the GPS/IMU integration and a digital elevation model. To remove the between-strip radiometric variations we propose to use a radiometric correction method, which is based on the information contained in the overlapping region of the image strips. The processing of data acquired by airborne multi-spectral scanner DAEDALUS *AADS 1268 ATM* show the effectiveness and potential of the proposed method especially for the thematic analysis applications.

1432-8364/03/2003/0317 $ 2.50

1 Introduction

Aerial survey of large areas with multispectral scanners requires the generation of image mosaics, which are usually composed of several image strips (Taylor 2001). The quality of the produced mosaic depends mainly on the radiometric and geometric characteristics of individual image strips after the correction.

Especially airborne data obtained from sensors having a wide field of view (e.g. up to 90 degrees) exhibit substantial viewing angle dependence of radiances across the image swath width due to illumination, atmospheric conditions, and BRDF of different objects. Usually these radiometric corrections are derived by physical modeling (Olbert 1998, Richter et al. 2002), which requires in-situ field and atmospheric measurements during the acquisition of the image data. Since in many cases such measurements are not performed simultaneously during aircraft overflight, empirical methods are necessary to achieve radiometrically homogeneous image data. Under the assumption of a stable and homogeneous atmosphere (justified for airborne data) the main radiometric distortions across an image strip are resulting from the variation of the sensor viewing angle (Staenz et al.1986, Kennedy et al. 1997). To perform relative normalization of these radiometric distortions within the image strip we are using an image-based empirical radiometric correction method EMRACO (Palubinskas et al. 2002, Palubinskas et al. 2003).

After the radiometric normalization the individual strips are ortho-rectified using our direct georeferencing software RECTIFY (Müller et al. 2002), which takes into account the following parameters: the exterior (measured by an IGI *CCNS*/*AERO contro-l IIb*) and interior orientation of the imaging system, the topography of the earth surface, the boresight misalignment angles between navigation sensor and camera system and the mapping coordinate reference system. One of the advantages of this approach in comparison with the conventional geometric transformation methods is that no ground control points are required.

Even if the individual image strips are radiometrically normalized, the seam line can be visible between the strips in the produced mosaic due to the change of the intensity and direction of solar illumination during the acquisition of adjacent image strips. Conventional mosaicking methods try to remove the between-strip radiometric variations by adjusting the mean, standard deviation values or histograms of the overlapping region. The seam line is drawn manually or goes through the tie points (e.g. found by using matching algorithm) (Afek & Brand 1998) in the overlapping region. We propose another radiometric correction method RADMOS, which is based on the unsupervised clustering in the overlapping region of the image strips. The mosaicking of two image strips is performed along the seam line, which is drawn along the boundaries of clusters. Thus a seamless mosaic can be created.

Each of these three steps of the mosaicking procedure are presented below in more detail followed by the application to airborne scanner data.

2 Radiometric Normalization

From general considerations of radiation transfer from the ground target to the sensor (under some assumptions) we can derive the empirical image-based radiometric correction method EMRACO (Palubinskas et al. 2002, Palubinskas et al. 2003), which corrects the radiances of pixels at the sensor for sensor viewing angle effects and indirectly for BRDF effects of the surfaces. The radiance at any viewing angle (off-nadir) is normalized to the radiance at the selected reference angle, usually in nadir direction. In order to implement such type of correction we need the objects (or classes or surface types) to be extracted from the image data.

We assume, that in some region of an image, around the reference angle (nadir), the pixel values are not or minimally distorted.

This assumption is valid for nadir-looking sensors.

This selected region of the image (usually symmetric on both sides of nadir) is used to initialize the whole procedure, which consists of several steps. First, the initial region of an image is clustered by an extended k-means algorithm, which defines automatically the number of clusters (classes) depending on the complexity of an image (Palubinskas 1999). Then for each cluster an average intensity profile along the scan direction is calculated. These profiles (initially defined in a central part of an image line) are extrapolated to the whole swath width of an image by a polynomial approximation. Finally, applying a linear regression method over all clusters to the radiation transfer equation results in a radiometric correction function for each sensor viewing angle with which the pixel intensity across the scan line can be relatively adjusted to the pixel intensity of the reference viewing direction. The procedure is iterative, that is the correction is first performed for a narrow central part of an image. Then the procedure is initialized with this corrected image region and repeated until the whole image swath width is corrected. This object-based correction method allows a relative correction of the local radiometric distortions.

3 Ortho-Rectification

The line scanner imagery are geometrically distorted with respect to a mapping frame. The upcoming high precision direct georeferencing systems consisting of a combined GPS/IMU and one or more imaging sensors can be used for orthoimage production provided a digital elevation model (DEM) is available in the case of single imagery. The utilization of direct measurements of the image exterior orientation parameters by a GPS/IMU system for image rectification is called Direct Georeferencing and allows a fast automatic ortho-rectification of the remotely sensed data. The basic concept of direct georeferencing, addressed by various authors in the last years (Bäumker & Heimes 2001, Cramer & Stallmann 2001, Ellum & El-Sheimy 2002, Grimm 2001, Jakobsen & Wegmann 2001, Mostafa 2001, Müller et al. 1999, Müller et al. 2002) is illustrated in Fig. 1.

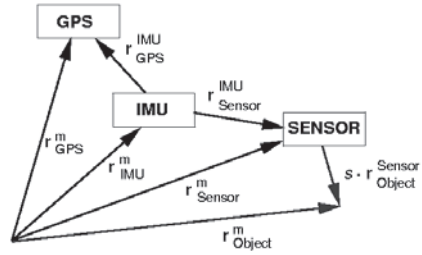

Fig. 1: Concept of direct georeferencing.

The collinearity concept is the basis for all direct georeferencing formulas, where the coordinates of an object point r^{Sensor}_{Object} measured in the imaging sensors coordinate frame are related to the coordinates r^{m}_{Object} in the mapping coordinate frame

$$r^{m}_{Object} = r^{m}_{Sensor} + s \cdot R^{m}_{IMU} R^{IMU}_{Sensor} \cdot r^{Sensor}_{Object}$$

with the actual position of the projection center of the sensor

$$r^{m}_{Sensor} = r^{m}_{GPS} - R^{m}_{IMU} \cdot r^{IMU}_{GPS} + R^{m}_{IMU} \cdot r^{IMU}_{Sensor}$$

The lower indices of the vectors r indicate the position of the points, whereas the upper indices denote the coordinate frame in which the vector is measured. The notation of the indices of the rotation matrices R indicates the transformation direction where the lower index represents the source system and the upper index the destination system. The meaning of the various parameters is explained in Tab. 1.

In a first step of the orthoimage production the six parameters of the exterior orientation (position and attitude data normally corrected by the lever arm calibration values) are synchronized with each image line. As input for the orthoimage processor serves the exterior orientation for each scan line, the model of the sensor (whiskbroom or pushbroom system) in combination with the calibrated interior orientation and a di-

Tab. 1: Definition of parameters for direct georeferencing.

m	Index which represents the mapping coordinate frame. For the mapping coordinate frame the unique cartesian coordinate system of a local topocentric system (LTS) with a fundamental point usually located at the center of an image strip can be used as intermediate coordinate frame (or in approximation a map projection like UTM). The position and attitude data have to be transformed to the mapping frame. But the resampling of the image tooks place in a map projection coordinate frame.
r^{m}_{Object}	Vector to the object point on the earth surface in the mapping frame, which has to be determined.
r^{Sensor}_{Object}	Vector from image point, which is measured by the sensor pixel location, to the corresponding object point on the earth surface in the sensor frame.
r^{m}_{Sensor}	Vector to the projection center of the sensor in the mapping frame, which is calculated using the integrated GPS/IMU data and the lever arm correction values measured during the hangar calibration procedure. Normally determined during postprocessing step.
R^{IMU}_{Sensor}	Rotation matrix between IMU and sensor coordinate frames, which accounts for possible tilt angles of the sensor mirror, stereo view angles and boresight misalignment angles (determined during calibration).
R^{m}_{IMU}	Rotation matrix between IMU and mapping coordinate frames, which is measured by the GPS/IMU system.
s	Scale factor determined by a DEM (or stereo processing techniques).
r^{m}_{GPS}	Measured vector to GPS antenna given in the mapping coordinate frame.
r^{IMU}_{GPS}	Vector from IMU to GPS measured in the IMU coordinate frame during hangar calibration (lever arm determination).
r^{IMU}_{Sensor}	Vector from IMU to sensor projection center measured in the IMU coordinate frame during hangar calibration (lever arm calibration values).
r^{IMU}_{Sensor}	Vector to IMU in the mapping coordinate frame, which is calculated using the integrated GPS/IMU data and lever arm corrections.

gital elevation model (DEM). Applying the rigorous collinearity equation the intersection point of each sensor look direction with the DEM is iteratively calculated. The resulting irregular grid is filled with bilinear interpolated pixel values. The orthoimage processor RECTIFY (Müller et al. 2002) supports a multitude of map projections (including local topocentric or ECEF coordinate systems) and geodetic datum transformations as well as ellipsoid to geoid transformations.

The boresight misalignment angles (the relation between IMU and sensor coordinate system) are determined by ground control points (calibration field) using an iterative least squares fit of the linearized collinearity equation.

For high quality direct georeferencing it is important to take into account all geometric parameters influencing the rectification process. Especially for sensors with a wide field of view the accuracy of the orthoimage is directly related to the accuracy of the used DEM.

For the accuracy assessment orthoimages of three different multispectral sensors (see Tab. 2) were investigated. The image data were acquired from the same test site located at DLR Oberpfaffenhofen.

An IGI *CCNS/AEROcontrol* with an IMU IIb (Grimm 2001) was used for the determination of the parameters of the exterior orientation. The manufacturer's instructions of the accuracy of the GPS/IMU system for the position is about 0.1–0.3 m

RMS using a GPS reference station and about 1–3 m RMS using the *OmniSTAR* satellite service. The accuracy for the heading angle is 0.1° and for the roll and pitch angle 0.01°.

The line scanners *ROSIS-03* and *DAIS 7915* were mounted together in the aircraft with the *CCNS/AEROcontrol*. The *Daedalus 1256* scanner was separately flown with the IMU directly mounted and aligned on the base plate of the scanner to minimize the boresight misalignment angles. The lever arm corrections were taken into account during postprocessing of the raw position and attitude data with the software delivered with the *CCNS/AEROcontrol* hardware resulting in the position of the projection centers of the scanners. Unfortunately the *OmniSTAR* service for the GPS position resulting in a position accuracy of 1–3 m RMS, was activated during the *Daedalus 1256* data acquisition resulting in worse position measurements than using a GPS reference station. For the *ROSIS-03* and *DAIS 7915* the reference station located on one of the roofs of the DLR buildings could be used with a position accuracy of about 0.1 m. For the synchronization of the elements of the exterior orientation with the image scan lines the PPS (Pulse per Second) of the GPS for *ROSIS-03* and *Daedalus 1256* was used, whereas *DAIS 7915* had an independent GPS clock. A DEM derived from the ERS-1/2 Tandem mission with 5–10 m vertical accuracy and 25 m horizontal resolution served as input for the rectification of the three images. The comparison of this DEM with a DEM (covering only partially the test site) derived from an aerial image stereo pair confirms the accuracy of the used DEM with mean height differences of about one meter measured at six corresponding points. The boresight misalignment angles were determined with 7 GCPs for *DAIS 7915* and *Daedalus 1256* and 5 GCPs for *ROSIS-03* well distributed over the scanned image area. The accuracy of the GCPs was better than 0.1 m. The comparison of the control points (also measured with DGPS) with the corresponding points manually measured in the orthoimages is listed in Tab. 3.

For the quality assessment the measurements were performed with pixel size accuracy (no subpixel measurement). For *DAIS 7915* five independent evaluators investigated the quality of the orthoimage with deviations of about 1m in the relative and absolute coordinates. The achieved geometric accuracy of the orthoimages for all three investigated sensors is in the range of 0.3 (*DAIS 7915*), 0.6 (*Daedalus 1256*) and 0.8 (*ROSIS-03*) pixel size.

For the *Daedalus 1256* scanner the moment of inertia of the mass of the rotating scan mirror leads to a non constant rotation speed during a roll movement which is corrected with a linear model resulting in an improvement of 0.95 m in the RMS values. Examples of the ortho-rectified scanner images of the three sensor types are shown in Fig. 2.

4 Radiometric Normalization Between Image Strips

To remove the radiometric variations between image strips we use the radiometric correction method RADMOS, which is

Tab. 2: Parameters of the three used airborne scanners.

Sensor	*ROSIS-03*	*DAIS 7915*	*Daedalus 1256*
Type	Pushbroom	whiskbroom	whiskbroom
FOV [°]	17.37	51.20	85.92
IFOV [mrad]	0.59	3.3	2.5
Altitude above ground [m]	3230	3230	2030
Ground resolution [m]	1.9	10.7	5.1

Tab. 3: Accuracy of the airborne orthoimages and the determined boresight misalignment angles.

Sensor	*DAIS 7915*		*ROSIS-03*		*Daedalus 1256*	
resolution [m]	10.7		1.9		5.1	
control points	22		12		21	
direction	north	east	north	east	north	east
absolute deviation [m]	2.69	− 2.22	1.43	− 0.04	− 0.05	− 3.03
RMS at GCP [m]	3.65	3.21	1.67	1.21	2.92	3.19
boresight misalignment (ω, φ, κ) [°]	− 0.375 0.867 − 0.479		− 0.399 − 1.317 0.140		0.419 0.242 − 0.049	

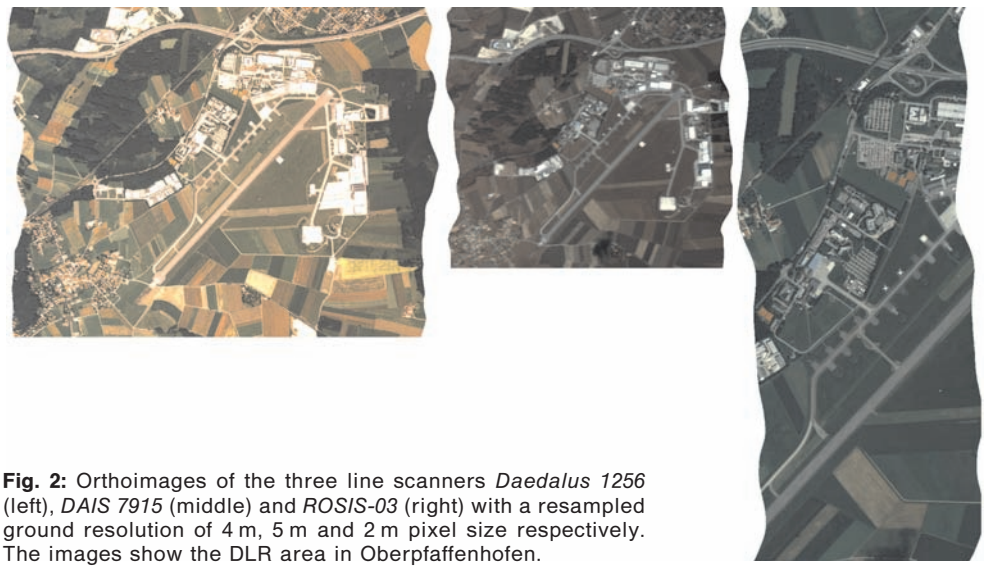

Fig. 2: Orthoimages of the three line scanners *Daedalus 1256* (left), *DAIS 7915* (middle) and *ROSIS-03* (right) with a resampled ground resolution of 4 m, 5 m and 2 m pixel size respectively. The images show the DLR area in Oberpfaffenhofen.

based on the information contained in the overlapping region of the images. First, the overlapping region is clustered by an extended k-means clustering algorithm, which automatically detects the different clusters (surface classes) in the region (PALUBINSKAS 1999). Then, the means of the clusters, calculated for each image strip separately, are used in the linear regression to derive the linear dependence between the radiances in the two image strips. This linear transformation is used for the radiometric normalization of image strips before the mosaicking. Finally, the mosaicking of two image strips is performed along the seam line, which is drawn along the boundaries of clusters, found after the unsupervised clustering in the overlapping region of the two image strips.

The whole mosaicking procedure is fully automatic and does not require any manual user interaction.

For the experiments the data acquired by airborne multi-spectral scanner *DAEDALUS AADS 1268* "Airborne Thematic Mapper" (ATM) were used. This DLR-own sensor is an opto-mechanical line scanner with 716 pixels in a line, an instantaneous field of view of 2.5 mrad and the total field of view of 86 degrees. At the altitude of 1000

meters it produces an image swath width of 1860 meters and a ground resolution of 2.5 meters. The data are recorded in eleven bands of the visible (5 channels), near- (3), middle- (2) and thermal- (1) infrared portions of the electromagnetic spectrum ranging from 0.4 to 13 µm.

In Fig. 3 (upper image) the mosaic created from five radiometrically unprocessed image strips (pseudo-color composite of bands: 0.45–0.52 µm, 0.63–0.69 µm and 0.91–1.05 µm) in the test site Gumattenkirchen (Bavaria) is shown. We can see clearly the radiometric distortions across the image strips due the sensor viewing angle effects and between-strips radiometric differences. The result of the proposed radiometric correction method is illustrated in the Fig. 4 (lower image), which shows a seamless radiometrically homogenous image mosaic.

Fig. 3: Mosaic of five image strips from multispectral scanner DAEDALUS *AADS 1268* (ATM) before radiometric correction (above) and after radiometric correction (below).

5 Applications

The range of applications comprises: integrating the orthoimage mosaics into digital topographic maps, thematic classification, data fusion, integrating all processing results into GIS and utilization of these data for 3D visualization. Some examples are given to show the potential of the generated image maps. All examples given have been acquired with the above mentioned Daedalus scanner.

The first example (Fig. 4) shows a part of an image mosaic of three flight strips in northern Germany (Havelburg), acquired shortly after the big flooding disaster of the river Elbe in August 2002, and integrated into a 1 : 25000 topographic map. The good fit of streets and linear features at the border lines between the orthoimage and the topographic map demonstrates qualitatively the high accuracy of the rectification process. The mouth of the river Havel into the river Elbe can be seen clearly as well as the regions which have been flooded two weeks before the data acquisition. The data are used to monitor the deposition of pollutants using ground truth measurements (taking samples). With the aircraft data a map of the different sediments can be produced to facilitate the sampling procedure and after the analysis of the samples to generate coverage maps of the pollutant distribution and wetness classes. The data are further used in a GIS.

The second example shows the use of an aircraft image mosaic in a data fusion project to search for indications of land mine areas in Croatia. In this project rectified and mosaicked Daedalus data (7 flight strips) are used in combination with radar data to clas-

sify different surface types, especially fallow areas, to show if demining actions can be supported by these means. A classified image resulting from the use of both data sets is shown in Fig. 5. Such a classification of the image mosaic could only be successful after the radiometric homogenization of the images and the image mosaicking explained in chapter 2 and 4.

The third example, Fig. 6, is a 3D visualization of an image mosaic which requires a high resolution DEM for it's generation. The perspective view can be easily calculated when orthoimages are used. After the flood of the river Elbe in August 2002 the City of Dresden has been covered by 15 flight stripes of the Daedalus scanner (ground resolution 1 m × 1 m/pixel). These data, as infrared composite, are superimposed over a laser DEM, supplied by the city authorities of Dresden for rectification purpose. Because of the high resolution DEM, the houses and trees can be seen as 3D objects. This shows that high resolution digital data are suitable for 3D visualization if the accuracy of the ortho-rectification is good enough even for high frequency height changes as the surface of a city.

Fig. 4: Part of an orthoimage mosaic (3flight strips) of the rivers Elbe and Havel about two weeks after the heavy floodings in August 2002, integrated into a topographic map.

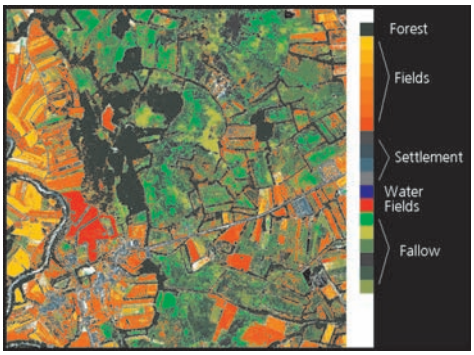

Fig. 5: Classification result with data fusion of optical (Daedalus, 3 flight strips) and radar data (E-SAR) for land mine area indication.

6 Conclusions

A mosaicking procedure is proposed which consists of three steps. First, the radiometric normalization of each individual image is performed using image-based empirical radiometric correction method EMRACO, which corrects for sensor viewing angle effects. Then the individual images are ortho-rectified using IGI navigation data with the direct georeferencing software RECTIFY. Finally, the seamless mosaic is created using radiometric correction method RADMOS, which removes the between-strip radiometric variations.

The whole mosaicking procedure is fully automatic and does not require any manual user interaction.

7 Acknowledgements

We would like to thank Beate Vollmer for the processing of many images/mosaics and for helping in improving the method. We also like to thank the office of environment (Umweltamt) Dresden for supplying a laser DEM of the city of Dresden.

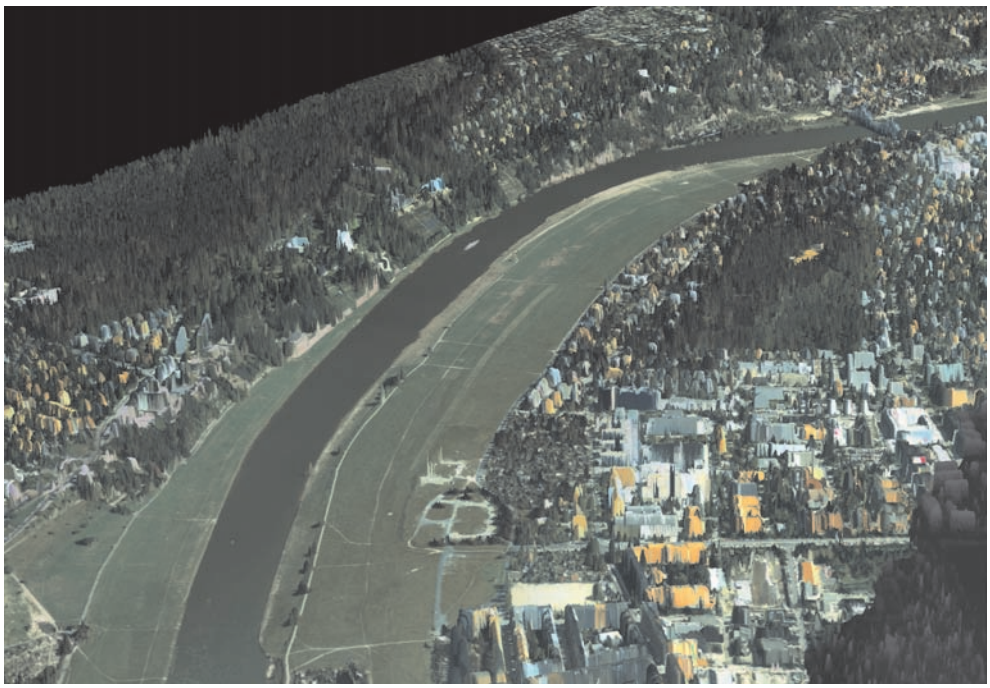

Fig. 6: Enlarged section of a 3D perspective view of the city of Dresden from ortho-rectified Daedalus images superimposed to a laser DEM. The original data set consists of 15 mosaicked flight strips. Presentation on the basis of laser scanner data, with authorization of the Land Surveying Office of Saxony. (DN V 74/02).

8 References

Afek, Y. & Brand, A., 1998: Mosaicking of orthorectified aerial images. – Photogrammetric Engineering & Remote Sensing **64** (2): 115–125.

Bäumker, M. & Heimes, F.J., 2001: New Calibration and Computing Method for Direct Georeferencing of Image and Scanner Data Using the Position and Angular Data of an Hybrid Inertial Navigation System. – OEEPE Workshop on Integrated Sensor Orientation. Hannover, Germany.

Cramer, M. & Stallmann, D., 2001: On the use of GPS/inertial exterior orientation parameters in airborne photogrammetry. – OEEPE Workshop on Integrated Sensor Orientation, Hannover, Germany.

Ellum, C. M. & El-Sheimy, N., 2002: Land Based Mobile Mapping System. – Photogrammetric Engineering & Remote Sensing, Jan. 2002, pp. 13–17.

Grimm, A., 2001: Results of the integrated CCNS AEROcontrol System. – OEEPE Workshop on Integrated Sensor Orientation, Hannover, Germany.

Jacobsen, K. & Wegmann, H., 2001: Dependencies and Problems of Direct Sensor Orientation. – OEEPE Workshop on Integrated Sensor Orientation, Hannover, Germany.

Kennedy, R.E., Cohen, W.B. & Takao, G., 1997: Empirical methods to compensate for a view-angle-dependent brightness gradient in AVIRIS imagery. – Remote Sensing of Environment **62:** 277–291.

Mostafa, M., 2001: Direct Georeferencing Column: An Introduction. – Photogrammetric Engineering & Remote Sensing, Oct. 2001, pp. 1105–1109.

Müller, Ru., Lehner, M., Reinartz, P. & Schroeder, M., 1999: Procedures for geometric rectification of airborne scanner data. – Proceedings of Workshop on Inorbit characterization of optical image systems. Bordeaux, France, 9 pages.

Müller, Ru., Lehner, M, Müller, Ra., Reinartz, P., Schroeder, M. & Vollmer, B., 2002: A program for direct georeferencing of airborne and spaceborne line scanner images. – Proceedings of ISPRS Commission I Mid-Term Symposium ''Integrating Remote Sensing at the Global, Regional and Local Scale''. Denver, CO, Vol. XXXIV, Part I, Commision I.

Olbert, C., 1998: Atmospheric correction for *casi* data using an atmospheric radiative transfer model. – Canadian Journal of Remote Sensing **24:** 114–127.

Palubinskas, G., 1999: An unsupervised clustering method by entropy minimization. – In: von der Linden, W., Dose, V., Fischer, R. & Preuss, R. (Eds.): Maximum Entropy and Bayesian Methods. – pp. 327–334, Dordrecht, Kluwer Academic.

Palubinskas, G., Müller, R. & Reinartz, P., 2002: Empirical radiometric correction of optical remote sensing imagery. – In: Shen, S.S. & Lewis, P.E. (Eds.): Algorithms and Technologies for Multispectral, Hyperspectral, and Ultraspectral Imagery VIII. – Proc. SPIE, Vol. 4725: 105–115.

Palubinskas, G., Müller, R. & Reinartz, P., 2003: Radiometric normalization of optical remote sensing imagery. – Proceedings of IGARSS'03 Symposium, Toulouse, France.

Richter, R., Müller, A. & Heiden, U., 2002: Aspects of operational atmospheric correction of hyperspectral imagery. – International Journal of Remote Sensing, **23**: 145–157.

Staenz, K., Meyer, P., Itten, K.I., Goodenough, D.G. & Teillet, P.M., 1986: Viewing angle corrections of airborne multispectral scanner data acquired over forested surfaces. – Proceedings of IGARSS'86 Symposium. Noordwijk, The Netherlands, vol. 1, pp. 671–676.

Taylor, G., 2001: Strategies for overcomming problems when mosaicking airborne scanner images. – Earth Observation Magazine, **10** (8): 26–31.

Addresses of the authors:

Rupert Müller, rupert.mueller@dlr.de

Gintautas Palubinskas,
gintautas.palubinskas@dlr.de

Peter Reinartz, peter.reinartz@dlr.de

Manfred Schroeder,
manfred.schroeder@dlr.de

Volker Amann, volker.amann@dlr.de

Rolf Stätter
Remote Sensing Technology Institute
German Aerospace Center DLR
Oberpfaffenhofen, D-82234 Wessling